THERMAL TIDES IN AN ASSIMILATION OF THREE YEARS OF THERMAL EMISSION SPECTROMENTER DATA FROM MARS GLOBAL SURVEYOR. R. J. Wilson[1], S. R. Lewis[2], and L. Montabone[2], [1]NOAA/Geophysical Fluid Dynamics Laboratory, Princeton, NJ 08542 (John.Wilson@noaa.gov), [2]Department of Physics & Astronomy, The Open University, Walton Hall, Milton Keynes MK7 6AA, UK.

Introduction. The thermal tides are planetary-scale gravity waves with periods that are harmonics of the solar day. Thermal tides are particularly prominent in the Mars atmosphere with the result that temperature and wind fields have a strong dependence on local solar time (LT). Tides include westward propagating migrating (sun-synchronous) waves driven in response to solar heating and additional nonmigrating waves resulting from zonal variations in the thermotidal forcing. Zonal modulation of forcing can arise from longitudinal variations of the boundary (topography and surface thermal inertia) and radiatively active aerosols (dust and water ice clouds). Nonmigrating tides appear as diurnally varying upslope/downslope circulations within the near-surface boundary layer that, like their migrating counterparts, are also able to propagate vertically to aerobraking altitudes in the lower thermosphere. The Mars Global Surveyor (MGS) Thermal Emission Spectrometer (TES) has yielded atmospheric temperature profiles with unprecedented latitude and longitude coverage that has provided the basis for characterizing the seasonal evolution of tides and stationary waves [1]. However, the twice-daily observations (2 am and 2 pm LT) are insufficient to unambiguously resolve the sun-synchronous tides. Recently the technique of data assimilation has been sufficiently developed for Mars to yield a dynamically consistent set of thermal and dynamic fields suitable for detailed investigations of various aspects of the martian circulations system [2,3,4,5]. We will refer to this data set an the TES reanalysis product, which represents the current best estimate of the evolving state of the martian atmosphere during the MGS mission. The assimilated thermal and dynamical fields provide a means of assessing circulation variability and transport capability reflecting the variability of the actual Mars atmosphere.

Data Assimilation: The data analysis was conducted by assimilating the TES temperature and column dust opacity retrievals into the Oxford Mars general circulation model (MGCM) to produce a physically self-consistent record of all atmospheric variables archived at a 2 hour interval over the entire MGS mapping period covering roughly three Martian years [2,3]. This data record includes the 2001 global dust storm and several large regional dust storms that occurred during the two other southern hemisphere summer seasons [6].

Three simulations are considered in this study. In addition to the full assimilation, we have examined a simulation using only the assimilated dust field without incorporating the TES temperatures. We have also examined a simulation with a specified dust distribution that roughly mimics a 'typical' MGS year. For this case, the assumed dust specification is zonally uniform. There is no information about the vertical dust distribution in the lower atmosphere from the nadir observations and so the model dust profile is specified by scaling an assumed (latitudinally and seasonally variable) dust profile by the observed column opacities [2,3].

The assimilated atmospheric fields may be readily decomposed into stationary waves, and eastward and westward propagating thermal tides (and traveling waves). We have examined the seasonal variation of the tide modes. We have looked at the evolving 3-D structure of temperature and geopotential, surface pressure, near-surface winds.

Thermal Tides: The longitude-time dependence of an arbitrary field in the fixed local reference frame typical for MGS observations may be represented as:

$$A(\lambda, t_{LT}) \sim \sum A_{s,\sigma} \cos[\,(s-\sigma)\lambda + \sigma t_{LT} + \delta_{s,\sigma}\,]$$

where s is the zonal wavenumber, λ is east longitude, σ is the temporal harmonic (σ=1 for the diurnal tide, σ=2 for the semidiurnal tide), t_{LT} is the local solar time, and $\delta_{s,\sigma}$ is the phase. Stationary waves are associated with σ= 0, tides with $s > 0$ ($s < 0$) propagate westward (eastward), and zonally symmetric tides have s= 0. The migrating tides ($s=\sigma$) have no longitude dependence in the sun-synchronous reference frame.

The latitudinal and vertical structure of the atmospheric response depends on both the period and structure of the forcing and on the efficiency of the atmospheric response to a given forcing. In the framework of classical tide theory, the westward propagating diurnal response may be represented by a series of equatorially confined, vertically propagating waves and vertically trapped waves in the extratropics. The simulated diurnal tide response is dominated by a vertically propagating component in the tropics with a vertical wavelength of about 33 km. Shorter vertical wavelengths are obtained for westward nonmigrating tides. The vertical wavelength of the tropical diurnal tide is of the order of the vertical smoothing length of the

TES nadir retrievals so that the observed amplitudes are notably reduced from the expected atmospheric response as represented by the reanalysis. By contrast, the extratropical tide response is characterized by relatively weak phase variation with height.

Tide theory indicates that the semidiurnal migrating tide response is dominated by a mode with a broad meridional structure and a very long vertical wavelength that efficiently responds to globally integrated dust heating. It has been demonstrated that the main features of the observed semidiurnal surface pressure oscillation at Viking Lander 1 (22°N) can be related to aerosol heating, at least during dusty periods [7]. This result is supported by the close correlation obtained between dust opacity and the simulated migrating semidiurnal tide in an earlier analysis of the assimilated surface pressure [8]. Figure 1 shows the seasonal variation of the migrating components of depth-weighted air temperature (T_{15}) centered at 0.5 mb (~25 km). This weighting yields a vertical smoothing that allows the assimilated temperature field to be readily compared with T_{15} synthesized from the TES data. The tide response reflects the effects of the regional dust storms in the first and third mapping years (MY24 and My26) and the global dust storm in MY25. There is a strong similarity in the tide responses to the 2001 global storm and the 1977a storm observed by the Viking orbiters.

Previous MGCM simulations have suggested that a rich mix of eastward and westward tide components is likely present at tropical latitudes and this is supported by our investigation of the TES reanalysis. The most prominent components of the eastward propagating, diurnal period response are the diurnal Kelvin waves (DK1, DK2,... corresponding to s=-1, -2, ...) which are meridionally symmetric and broad solutions of the Laplace Tidal Equation. DK1 has a vertical structure that closely corresponds to the equivalent barotropic Lamb wave and may be resonantly enhanced [9]. DK2 and DK3 are vertically propagating modes with wavelengths of roughly 90 and 50 km, respectively, and have amplitudes that increase exponentially with height. Long vertical wavelengths render these Kelvin waves less susceptible to thermal dissipation than the shorter westward propagating modes, allowing them to appear prominently in the upper atmosphere [10,11,12]. By contrast, the nonmigrating westward modes include tropically confined modes with relatively short vertical wavelengths and a second group of mid and high latitude modes that are vertically trapped. Nonmigrating semidiurnal tides also have long vertical wavelengths and evidently contribute to the observed thermospheric density variations [11,12,13].

We have examined longitude-height sections of simulated zonal wave 2, 3 and 4 components of tropical temperature (and geopotential) and found that they may be interpreted as the superposition of eastward propagating Kelvin modes with long vertical wavelengths and westward propagating waves with much shorter wavelengths. TES limb retrievals suggest similar structures, but the shorter westward propagating waves are evidently more strongly attenuated due to the finite vertical resolution.

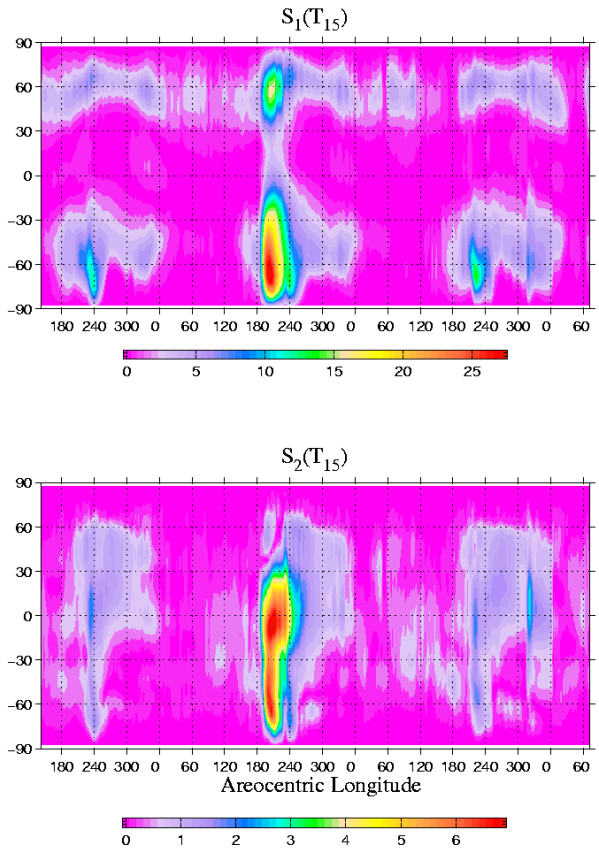

Figure 1. Seasonal variation of the migrating diurnal (top) and semidiurnal (bottom) components of midlevel (0.5 mb) temperature. The influence of the 2001 global dust storm is particularly prominent.

TES nadir results are also consistent with this description, but show the influence of even greater vertical averaging, so that only the long Kelvin waves are evident. Density variations are dominated by the effect of vertically integrated temperature and would tend to reflect the presence of the long Kelvin waves. In fact, measurements obtained during Phase 2 of MGS aerobraking have revealed large amplitude, planetary-scale longitudinal variations in dayside density at 130 km, with zonal waves 2 and 3 being particularly prominent for ± 60° latitude. It has been concluded that eastward propagating nonmigrating tides could account for

much of the planetary scale wave structure observed in MGS accelerometer density data (in a fixed local time reference) [11,12,13]. The observed wave 3 density variation was largely attributed to a wave 2 diurnal Kelvin mode (DK2) in the tropics and an eastward-propagating wave 1 semidiurnal tide at extratropical latitudes.

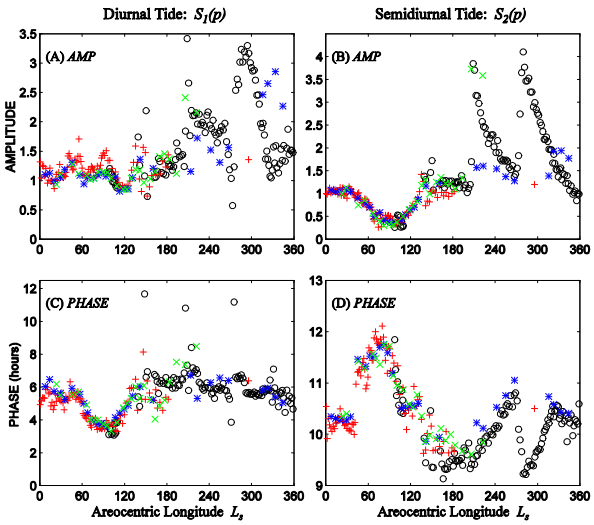

Figure 2. The seasonal variation of diurnal (left) and semidiurnal (right) tides derived from the 4 year record of surface pressure at the Viking Lander 1 site (22°N, 312°E). Tide amplitudes are normalized (%) by the diurnal-mean surface pressure.

Viking Lander Comparison: The time series of surface pressure observations by the two Viking Landers allows for an interesting comparison with the assimilated surface pressures. The Viking Lander 1 tide record shown in Figure 2 suggests a high degree of repeatability for 4 Mars years in the L_s=0-130° season. This absence of interannual variability is consistent with the TES temperature record [Smith], suggesting that it is reasonable to make the comparison between the two missions. Systematic seasonal variations in phase and amplitude of the diurnal and semidiurnal surface pressure tides at the two Viking Lander sites are consistent with the presence of resonantly enhanced wave 1 diurnal and wave 2 semidiurnal Kelvin waves [*9,14*]. These waves were shown to be forced by dynamical effects induced by topography.

Figure 3 shows the corresponding surface pressure variations from the TES reanalysis. The assimilated semidiurnal tide amplitude is somewhat weak compared to Viking during the relatively clear seasons, while there is good agreement in the tide phase. This latter agreement suggests that relative amplitudes of the semidiurnal migrating and Kelvin wave response are reasonably correct. The semidiurnal tide amplitude for the 2001 global dust storm is comparable to the peaks observed during the 1977a and 1977b dust storms.

The agreement between the diurnal tide component is less good. In particular, the assimilated tide phase is much more variable during the L_s=30-120 season and the amplitude suffers a pronounced decline by L_s=120

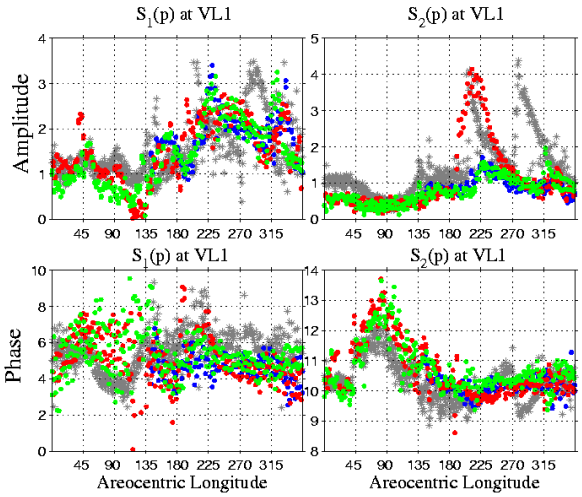

Figure 3. A comparison of the assimilation tides with those observed at the VL1 site (see Fig. 1). The observed tides are shown in gray (see Fig. 1).. seasonal variation of diurnal (left) and semidiurnal (right) tides derived from the 4 year record of surface pressure at the Viking Lander 1 site (22°N, 312°E).

The main contributors to the surface pressure response at the latitude of VL1 (22°N) are shown in Figure 4. Results from the reanalysis, control and zonally-uniform dust simulations are shown. The variable phase throughout the L_s =30-120 period and amplitude drop-out at L_s = 120 can be attributed to the variations in the phase and amplitude of the diurnal Kelvin wave. The tide response at the VL1 site is a result of constructive interference between the eastward and westward propagating tide modes. In particular, the amplitude of the diurnal Kelvin wave in the reanalysis declines significantly compared with the response in the control simulation. The diurnal migrating tide response is not much changed by the "forcing" of the MGCM by the TES temperatures. The Kelvin wave will respond to changes in the zonal variation in tide forcing, particularly the zonal wave 2 structure. We speculate that the variable phase in the reanalysis reflects the influence of water ice cloud radiative forcing that may

be implicit in the "forcing" by the TES temperature retrievals. Recent observations and modeling work have indicted that nighttime water ice clouds, with a strong wave 2 distribution, can have a significant radiative impact. This effect is not currently represented in the MGCM, and so would not be present in the control run. The reanalysis does not reflect the presence of strong inversions that were found in early morning (0400 LT) tropical temperature profiles derived from Radio Science occultations [15]. These inversions have been attributed to radiatively active water ice clouds, which can enhance the forcing of tropical nonmigrating tides [15].

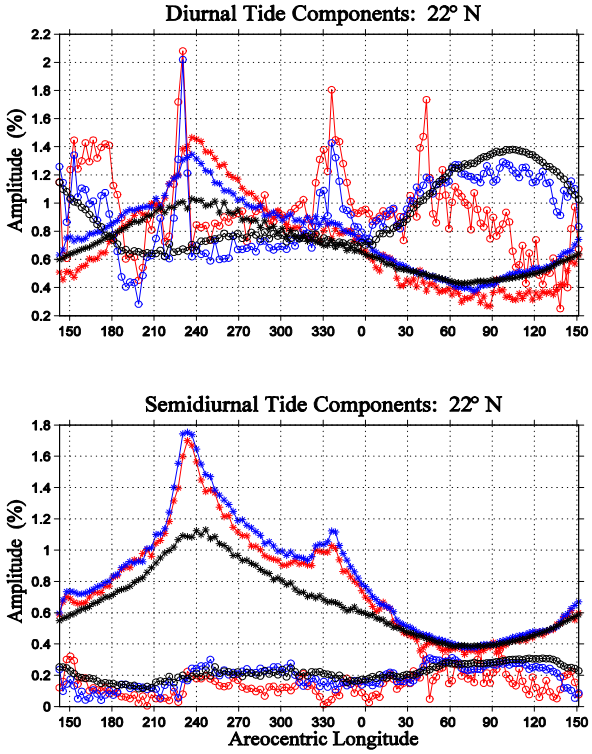

Figure 4. Seasonal variation of the two main diurnal (top) and semidiurnal (bottom) components of surface pressure at 22° N. The migrating tide is shown with stars while the Kelvin waves are indicated with open circles. Results from the TES reanalysis are shown in red, while the control run are shown in blue and the smooth dust case is shown in black.

Future work: We are continuing to relate diurnal variations in many of the fields to changes in radiative heating and in the circulation. A comparison of atmospheric temperatures in the reanalysis and control runs may provide insight into systematic biases in the model. Figure 5 shows the difference in equatorial zonal mean temperature between the reanalysis and control simulations. The warming response to the TES "forcing" during the L_s=60-150 season may reflect the radiative influence of tropical water ice clouds [16]. Of course, biases in the assumed vertical distribution of dust or the Hadley circulation response are other possibilities..

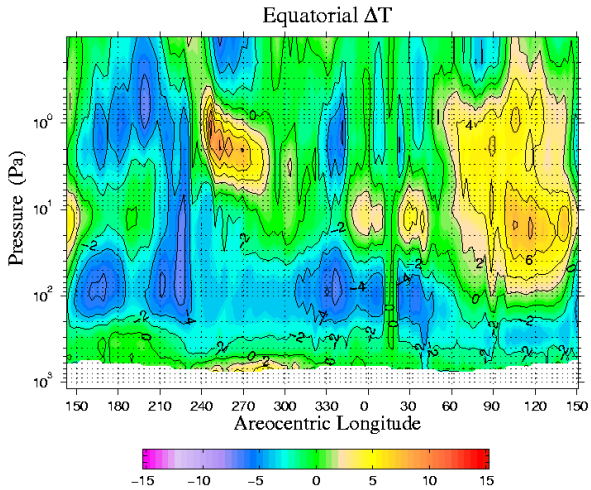

Figure 5. Seasonal variation of the difference between the equatorial zonal mean temperature for the TES reanalysis and control simulations. The incorporation of TES temperature retrievals yields a warmer atmosphere during the northern hemisphere summer solstice season.

References: [1] Banfield, D. et al. (2003) *Icarus*, 161, 319-345. [2] Montabone, L. et al. (2005) *Adv. Space Res.*, *36*, 2146-2155. [3] Montabone, L. et al. (2006) *Icarus*, *185*, 113-132. [4] Lewis, S.R. et al. (2007) *7th International Conference on Mars*. [5] Montabone, L. et al. (2007) *7th International Conference on Mars.* [6] Smith, M.D. (2004) *Icarus*, *167*(1), 148-165. [7] Zurek, R.W. and C.B. Leovy (1981), *Science*, *213*, 437-439. [8] Lewis., S.R., and P.R. Barker (2005) *Adv. Space Res.*, 36, 2162-2168. [9] Wilson, R.J. and K.P. Hamilton (1996) *J. Atmos. Sci.*, **53**, 1290-1326. [10] Wilson, R.J. (2000) *Geophys. Res. Lett.*, *27*, 3889-3892. [11] Wilson, R.J. (2002) *Geophys. Res. Lett.*, *29*, 10.1029/2001GL013975. [12] Withers, P. et al. (2003) *Icarus*, *164*, 14-32. [13] Angelats i Coll., M. et al. (2004) *JGR*, *109*, E01011, doi:10.1029/2003JE002163. [14] Bridger, A.F.C., and J.R. Murphy (1998) *J. Geophys. Res.*, *103*, 8587-8601. [15] Hinson, D. and R.J. Wilson (2004) *JGR*, *109*, E10002, doi:10.1029/JE002129. [16] Wilson, R.J. et al. (2007) *Geophys. Res. Lett.*, *34*, L02710, doi:10.1029/2006GL027976.